Wright State University
CORE Scholar

Physics Faculty Publications | Physics

6-1-2010

Magnetotransport Properties of High Quality Co:ZnO and Mn:ZnO Single Crystal Pulsed Laser Deposition Films: Pitfalls Associated with Magnetotransport on High Resistivity Materials

John S. McCloy

Joseph V. Ryan

Timothy C. Droubay

Tiffany C. Kasper

Scott A. Chambers

See next page for additional authors

Follow this and additional works at: https://corescholar.libraries.wright.edu/physics

Part of the Physics Commons

Repository Citation
McCloy, J. S., Ryan, J. V., Droubay, T. C., Kasper, T. C., Chambers, S. A., & Look, D. C. (2010). Magnetotransport Properties of High Quality Co:ZnO and Mn:ZnO Single Crystal Pulsed Laser Deposition Films: Pitfalls Associated with Magnetotransport on High Resistivity Materials. *Review of Scientific Instruments, 81* (6), 63902.
https://corescholar.libraries.wright.edu/physics/176

This Article is brought to you for free and open access by the Physics at CORE Scholar. It has been accepted for inclusion in Physics Faculty Publications by an authorized administrator of CORE Scholar. For more information, please contact corescholar@www.libraries.wright.edu, library-corescholar@wright.edu.

Authors
John S. McCloy, Joseph V. Ryan, Timothy C. Droubay, Tiffany C. Kasper, Scott A. Chambers, and David C. Look

This article is available at CORE Scholar: https://corescholar.libraries.wright.edu/physics/176

Magnetotransport properties of high quality Co:ZnO and Mn:ZnO single crystal pulsed laser deposition films: Pitfalls associated with magnetotransport on high resistivity materials

John S. McCloy,[1] Joseph V. Ryan,[1] Timothy Droubay,[2] Tiffany C. Kaspar,[2] Scott Chambers,[2] and David C. Look[3]
[1]*Energy and Environment Directorate, Pacific Northwest National Laboratory, Richland, Washington 99354, USA*
[2]*Fundamental and Computational Sciences Directorate, Pacific Northwest National Laboratory, Richland, Washington 99354, USA*
[3]*Semiconductor Research Center, Wright State University, Dayton, Ohio 45434, USA*

(Received 25 March 2010; accepted 25 April 2010; published online 17 June 2010)

The electrical resistivity values for a series of pure and doped (Co, Mn, Al) ZnO epitaxial films grown by pulsed laser deposition were measured with equipment designed for determining the direct current resistivity of high resistance samples. Room-temperature resistances ranging from 7×10^{1} to 4×10^{8} Ω/sq were measured on vacuum-reduced cobalt-doped ZnO, (Al,Co) co-doped ZnO, pure cobalt-doped ZnO, Mn-doped ZnO, and undoped ZnO. Using a four-point collinear geometry with gold spring-loaded contacts, resistivities were measured from 295 to 5 K for resistances of $<\sim10^{12}$ Ω/sq. In addition, magnetoresistance and Hall effect were measured as a function of temperature for select samples. Throughout the investigation, samples were also measured on commercially available instrumentation with good agreement. The challenges of transport measurements on high resistivity samples are discussed, along with some offered solutions to those challenges. © *2010 American Institute of Physics.* [doi:10.1063/1.3436648]

I. INTRODUCTION

Zinc oxide (ZnO) is a transparent semiconducting oxide which has been extensively studied for a wide variety of electronic, optoelectronic, and magnetoelectronic applications. Room-temperature electrical conductivity in ZnO can vary by at least ten orders of magnitude, depending on purity and electronic doping levels. In its high-conductivity state, ZnO has been used in transparent thin-film transistors,[1–3] components of solar cells,[4] and transparent contacts for various kinds of displays.[5] Doping with 3*d* transition metal ions such as Co and Mn has been predicted to be a means of producing dilute magnetic semiconductor ZnO where the spins are coupled to the electronic states.[6,7] However, recent work exploring various Co:ZnO with various carrier concentrations failed to demonstrate carrier-mediated room-temperature ferromagnetism, contrary to the mean-field theory prediction.[8] In spite of this, the prospect of achieving highly dense random access memories through spintronic devices has motivated continued work.

The defect types and majority carrier concentrations in ZnO vary greatly according to how the ZnO is prepared, even without deliberate dopants. Bulk-crystal ZnO room-temperature resistivity varies substantially from 10^{-1} Ω-cm in vapor-phase grown crystals[9] to 10^{2} Ω-cm for hydrothermally synthesized crystals.[10] Higher resistivities up to 10^{6} Ω-cm are obtainable from hydrothermal synthesis due to unintentional doping with Li or K, which are present as hydroxides in the hydrothermal process.[11] Theoretically, high resistivities are indicative of high purity and crystallographically well-ordered crystals and films, but in practice high resistivity is only obtained when certain conditions are met for the defect population of shallow donors ($N_{D,\text{shallow}}$), deep donors ($N_{D,\text{deep}}$), shallow acceptors ($N_{A,\text{shallow}}$), and deep acceptors ($N_{A,\text{deep}}$). Specifically, high-resistivity material is obtained when $N_{D,\text{shallow}}<N_{A,\text{shallow}}$ and $N_{D,\text{deep}}>(N_{A,\text{shallow}}-N_{D,\text{shallow}})$, or when $N_{A,\text{shallow}}<N_{D,\text{shallow}}$ and $N_{A,\text{deep}}>(N_{D,\text{shallow}}-N_{A,\text{shallow}})$. The complex nature of defect self-compensation in ZnO underlies the difficulty of achieving *p*-type ZnO material.[12,13] Typical shallow donors for single-crystal ZnO are believed to be zinc interstitials, oxygen vacancies, hydrogen impurities, and group III metal impurities, particularly aluminum. Low resistivity films on the order of 10^{-2}–10^{-3} Ω-cm are readily obtained by many methods by using low oxygen pressures.[6] However, very high room-temperature resistivities on the order of 10^{9} Ω-cm have been achieved in thin films grown under high oxygen pressure.[14] The ability to measure electronic transport in ZnO enables distinctions between intrinsic and defect/impurity induced phenomena. Measurements of high-resistivity, wide band gap materials are notoriously difficult. Detailed analyses of the relationships between purity and structural perfection and conductivity have only been made for a few systems.[15,16]

Here, we present results on electrical measurements in thin films with sheet resistances up to 10^{12} Ω/sq (film resistivities of at least 10^{9} Ω-cm) using a buffered voltage measurement combined with a current source stable to below 1 pA. Direct current measurements of such high resistivities present unique challenges, as very low applied currents and extremely long wait times may be required to ensure that equilibrium voltages are reached in the presence of poten-

 © 2010 American Institute of Physics

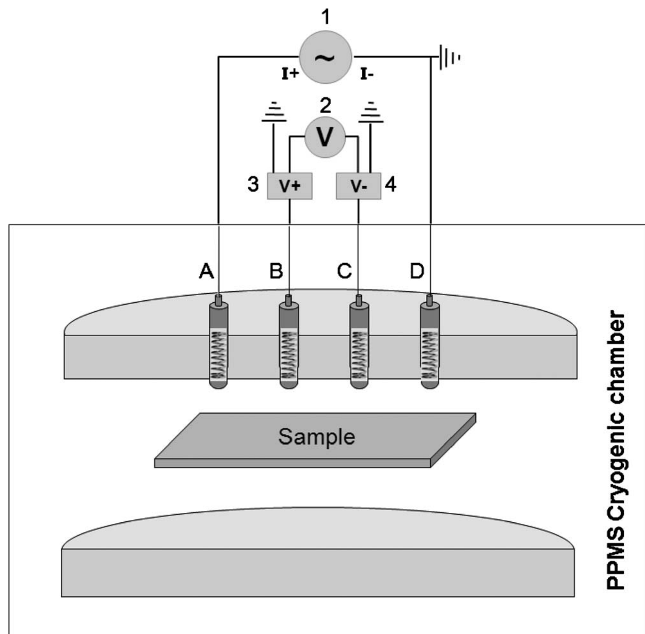

FIG. 1. A schematic of the buffered resistivity measurement system used in the PPMS. Numbers and letters are defined in the text.

tially large capacitances in series with large material resistances. We have conducted measurements on ZnO samples requiring a range of seven orders of magnitude in the applied current and representing a resistance range of over ten orders of magnitude. The goal was to produce a system for research that had maximum flexibility for thin-film sample measurements (e.g., spring-loaded contacts), easily measure very high resistivities $>10^{10}$ Ω-cm, and be easily reproduced. In the process of this development, many questions were answered including (1) the importance of the contact method (pin contact and soldered wire), (2) the role of time constant in cabling {RC [Resistance (R)×Capacitance (C)] transient}, (3) the importance of the method [four-point collinear versus van der Pauw (VDP) configuration] and geometrical corrections, (4) the size of the signal relative to noise, and (5) the importance of establishing a true zero in the magnetic field.

II. EXPERIMENTAL METHODS

A. Electrical transport apparatus

Film resistivities were determined in multiple ways in order to cross-check and validate results. At room temperature, a bench top four-point-collinear probe apparatus (Keithley 2400 sourcemeter) with tungsten carbide spring contacts was used for initial measurements, especially for the lower resistivity samples. Resistivity, Hall, and magnetoresistance (MR) measurements were then taken in the temperature range of 5–295 K, and in magnetic fields up to 9 T, using a physical property measurement system (PPMS) (Quantum Design, San Diego, California).

For samples generating raw resistance values greater than 1 MΩ, the standard electronics of the PPMS are insufficient. Therefore, an alternative electrical measurement apparatus was designed and utilized and is depicted in Fig. 1. A subfemtoamp source meter (Keithley 6430, 1 in Fig. 1) was used to supply a known current between two pins. The voltage drop between source pins A and D (called V_{source}) was measured as a check to other data points, and is essentially a two point resistivity measurement. Per suggestions from Keithley Instruments (Cleveland, Ohio),[17] the voltage measurements for both geometries utilized in the experiments (VDP and four-point collinear) were protected from common leakage currents through the use of two electrometers (Keithley 6512 and 6514, 3 and 4 in Fig. 1) run in guarded mode serving as unity gain buffers. This type of circuit essentially produces a duplicate of the voltage to be measured while preventing the injection of current into the system, ensuring that the measurement will not affect the rest of the circuit. The difference between these two electrometers, corresponding to the voltage between pins B and C (called V_{drop}), was determined using an Agilent 34401A (Santa Clara, California) digital multimeter (2 in Fig. 1). A custom graphical interface code was written to integrate the operation of the PPMS with the various electrical measurement devices. Guarded coaxial or triaxial cabling was used throughout the signal path to reduce electromagnetic interference and capacitance delays.

In addition, temperature-dependent Hall effect measurements from 15 to 320 K were carried out on some of the samples at Wright State University (WSU) using a Lakeshore (LS) model 7507 apparatus at 0 and 1 T fields. Samples were immersed in He exchange gas during measurement to stabilize the temperature. Thermometer accuracy was better than 0.1 K and magnetic field accuracy was better than 10^{-4} T. Ohmic contacts were achieved by soldering small dots of indium onto the corners of the sample and connecting with copper wires in the VDP configuration.

B. Sample preparation

Pulsed laser deposition (PLD) was used to deposit epitaxial thin films of $Co_xZn_{1-x}O$, $Mn_xZn_{1-x}O$, (Co, Al):ZnO, and pure ZnO on Al_2O_3 (sapphire) substrates; *a*-plane ZnO(1120) was obtained on *r*-plane $Al_2O_3(1-102)$ and *c*-plane ZnO(0001) was obtained on *c*-plane $Al_2O_3(0001)$. To minimize the deposition of molten droplets and particles during the laser ablation process, an off-axis growth configuration was utilized. All growths were performed in 10 mTorr of O_2 unless otherwise noted. Pressure was controlled using a combination of a mass flow controller and an automatically throttled gate valve between the chamber and the primary system turbopump. A KrF laser (248 nm, 2.4 J cm^{-2}, and 1–20 Hz) was rastered across a rotating target. The substrate holder was also rotating which, along with laser rastering and target rotation, provided uniform deposition across the substrate. Different targets were used to incorporate the desired dopant(s) at the desired concentration(s). These included targets processed from $Mn_{0.05}Zn_{0.95}O$ and $Co_{0.04}Zn_{0.96}O$ colloidal nanoparticles,[18,19] combustion synthesized Al-doped ZnO nanoparticles,[20] and targets prepared using the more conventional route of thoroughly mixing commercially available powders of ZnO and CoO to make a $Co_{0.10}Zn_{0.90}O$ target. The starting target materials were mixed with small amounts of de-ionized water and polyethylene glycol binder, cold pressed, and sintered for 4–6 h at

TABLE I. Pulsed laser deposited thin film parameters. Thicknesses determined by x-ray reflection (XRR), optical profilometry (profil.), or Rutherford backscattering (RBS). PLD targets were either conventional (conv) or nanoparticle (nano) as described in the text.

Sample ID	Substrate	Cat% M	Cat% Al	Thickness (nm)	Target	Substrate temperature (°C)	O_2 press	Vacuum anneal
111307R	*r*-sapphire	6.2 (Co)	~1	64.6 (XRR) 84.0 (profil.)	Conv Co:ZnO+Al:ZnO	400	Vacuum	None
112107AR	*r*-sapphire	3.7 (Co)	⋯	274 (RBS) 276.9 (profil.)	Nano Co:ZnO	550	10^{-2} Torr	700 °C/4 h
081006E	*c*-sapphire	5.0 (Mn)	⋯	3271.7 (profil.)	Nano Mn:ZnO	550	5×10^{-2} Torr	None
102507C	*c*-sapphire	14.6 (Co)	⋯	405.6 (RBS) 429.9 (profil.)	Conv Co:ZnO	400	$\sim10^{-7}$ Torr	None
063009	*c*-sapphire	⋯	⋯	3285 (profil.)	Conv ZnO	550	10^{-2} Torr	None

1000 °C in air. All targets were preablated in oxygen prior to every deposition to remove surface contaminants. In addition, substrates were heated up to the growth temperature in 10 mTorr O_2 to remove adventitious carbon from the substrate surface prior to growth. Specific processing details are shown in Table I. When co-doping, or seeking a stoichiometry other than that of the individual targets, the film composition was varied by combining laser pulses from the different targets in various proportions under computer control. For these cases, in which ablation is occurring sequentially from different targets, the laser repetition rate was lowered from 5 to 1 Hz. In contrast, a laser repetition rate of 5 Hz was typically used for growths from single targets. The co-doped films were thus carried out at a slower overall deposition rate and the sequence included many short periods with no deposition (during target changeover). Periods of no deposition with the substrate at elevated temperatures resulted in enhanced dopant concentrations relative to periods with more frequent pulses due to preferential re-evaporation of Zn. Additional details concerning the preparation of Co^{2+}:ZnO (Ref. 19) and Mn^{2+}:ZnO (Ref. 18) colloidal nanoparticles and characterization of $Co_xZn_{1-x}O$ (Ref. 8) and $Mn_xZn_{1-x}O$ (Ref. 21) PLD-grown films have been described elsewhere.

III. RESULTS

A. Resistivity

Film resistivities were measured using multiple instruments and methods to validate the measurements on the buffered electrometer configuration, as summarized in Table II. First, thin films were measured at room temperature using the bench-top, four-point collinear method. Samples were then measured as a function of temperature in the PPMS from approximately 295 to 5 K using the specially designed four-point collinear gold spring contacts (Fig. 2). Samples were measured using several currents each to establish the acceptability of the contact (Ohmic versus Schottky). A summary of all the temperature dependent resistivity data, where contacts were verified as Ohmic, is shown in Fig. 3.

In three cases ($Zn_{0.928}Co_{0.062}Al_{0.01}O$, $Zn_{0.963}Co_{0.037}O$, and $Zn_{0.95}Mn_{0.05}O$) both VDP and four-point COL measurements were performed. $Zn_{0.928}Co_{0.062}Al_{0.01}O$ was tested with both soldered wires (s) and pin contacts (p) in the PPMS. $Zn_{0.95}Mn_{0.05}O$ was tested in the PPMS with pin contacts in both the VDP and COL configurations (Fig. 4). Two of the samples ($Zn_{0.963}Co_{0.037}O$ and $Zn_{0.928}Co_{0.062}Al_{0.01}O$) were also measured with soldered contacts in the VDP configuration on the LS system.

B. Hall effect

Temperature dependent Hall measurements were conducted at 0 and 1 T in the VDP configuration on $Zn_{0.963}Co_{0.037}O$ and $Zn_{0.928}Co_{0.062}Al_{0.01}O$ at WSU on the LS system (Fig. 5), and room-temperature Hall effect was measured for $Zn_{0.95}Mn_{0.05}O$. All measurements performed at WSU had indium-soldered contacts at the edges of the films. On the PPMS, temperature-dependent Hall measurements of $Zn_{0.95}Mn_{0.05}O$ at 3 and 6 T were made down to 125 K using the pin contacts which were inset from the corners (see Fig. 6). Due to small signals, the data were only reliable for calculating mobilities and carrier concentrations down to 205 K at 3 T data and 165 K at 6 T. Hall coefficient, electron mobility, and electron concentration were computed from these data (see Table III). All materials were found to be *n*-type.

TABLE II. Comparison of resistivities collected different ways. Values in parentheses indicate applied currents used to measure resistivity. (VDP indicates Van der Paw geometry, COL indicates four-point collinear geometry, "s" indicates soldered contacts, and "p" indicates pin contacts. PPMS is the physical property measurement system and LS is the Lakeshore system.)

Sample ID	Material	Resistivity (Ω-cm) (RT, bench top)	Resistivity (Ω-cm) (295 K, COL unless noted, PPMS)	Resistivity (Ω-cm) (5 K, COL unless noted, PPMS)	Resistivity (Ω-cm) (RT, VDP, LS)
111307R	$Zn_{0.928}Co_{0.062}Al_{0.01}O$	4.7×10^{-4}	3.0×10^{-4} (VDP, s) 4.65×10^{-4} (COL, 70.5 mA, p)	2.5×10^{-4} (VDP, s) $<3.89\times10^{-4}$ (COL, 70.5 mA, p)	3.49×10^{-4} (1 mA, s)
112107AR	$Zn_{0.963}Co_{0.037}O$	4.7×10^{-1}	9.00×10^{-1} (200–600 nA, p)	1.36×10^{2} (200–600 nA, p)	2.02×10^{0} (10 μA, s)
081006E	$Zn_{0.95}Mn_{0.05}O$	⋯	1.27×10^{0} (VDP, 1 mA, p) 2.43×10^{0} (COL, 1–3 mA, p)	5.73×10^{8} (VDP, 1 mA, p) 1.02×10^{9} (COL, 1–3 mA, p)	1.33×10^{0} (100 μA, s)
102507C	$Zn_{0.854}Co_{0.146}O$	1.2×10^{3}	1.09×10^{2} (5–105 nA, p)	$>10^{9}$ (5–75 pA, p)	⋯
063009	Undoped ZnO	⋯	1.3×10^{5} (30–50 pA, p)	$>10^{9}$ (30–50 pA, p)	⋯

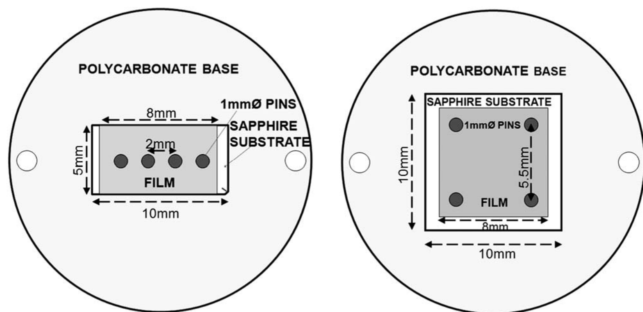

FIG. 2. A schematic of the four-point collinear (COL) pin contacts (left) and the VDP pin contacts (right).

C. MR

For the $Zn_{0.963}Co_{0.037}O$ and $Zn_{0.928}Co_{0.062}Al_{0.01}O$ samples, MR versus temperature at 1 T was measured at WSU using soldered contacts, while MR at 2 K versus field from 0 to 9 T was performed on the PPMS at Pacific Northwest National Laboratory in Richland, Washington, using pin contacts (Fig. 7).

The low temperature measurements of the $Zn_{0.928}Co_{0.062}Al_{0.01}O$ sample showed consistent results as a function of field and applied current, and contacts were shown to be Ohmic. However, for the $Zn_{0.963}Co_{0.037}O$ sample, it was determined that pin contacts were no longer Ohmic for this measurement, and the high resistivity caused difficulties with cabling time constants and the associated voltage drift.[22] Our experience with this measurement caused us to redesign the cabling system with a goal of minimizing or eliminating the cabling capacitance.

IV. DISCUSSION

The goal of our investigation was twofold: (1) to develop a reliable and robust experimental apparatus for measuring resistivity and magnetotransport of highly resistive samples of ZnO and other wide band-gap oxides, and (2) to explore the phenomenology of the magnetotransport in magnetically-doped ZnO epitaxial films. In what follows, we discuss the lessons learned from our multiple measurements and analyze the data to gain insight into the materials.

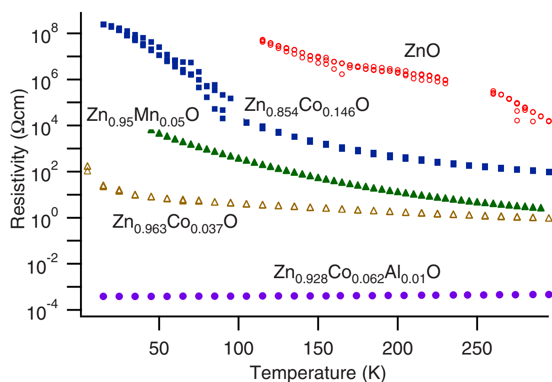

FIG. 3. (Color online) Summary of resistivity vs temperature on ZnO samples.

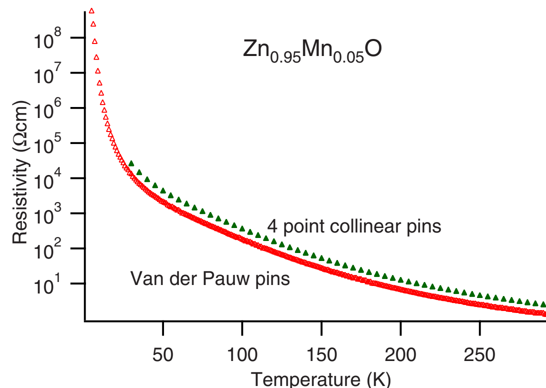

FIG. 4. (Color online) Comparison of resistivity of $Zn_{0.95}Mn_{0.05}O$ using VDP and COL pin geometries.

A. Experimental protocol

1. Contacts and geometry

The development of noninvasive, reliable, and reproducible contacts was a major consideration in the design of the apparatus. Part of the motivation for testing with different instruments and contacts was to assess the viability of unsoldered contacts. To test this, contacts to the film surfaces were made by spring-loaded gold pins (PPMS) or by indium solder and silver (PPMS) or copper (LS) wires. The pins were press fitted through a polycarbonate puck in the orientation desired (COL or VDP), wires were soldered to the tops of the pins, and the samples were squeezed between a base plate and the spring pin polycarbonate block using two screws.

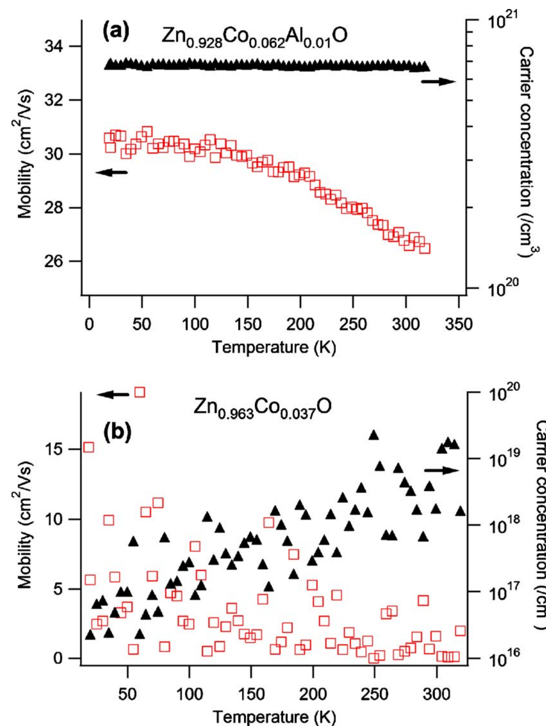

FIG. 5. (Color online) Mobility and carrier concentration of (a) $Zn_{0.928}Co_{0.062}Al_{0.01}O$ and (b) $Zn_{0.963}Co_{0.037}O$ from 1 T Hall experiment with soldered contacts. Open squares are mobility and solid triangles are carrier concentration. Note that the Hall voltages for the $Zn_{0.963}Co_{0.037}O$ sample (b) were sufficiently low with a 1 T field and that the determined values of mobility and carrier concentration are very noisy.

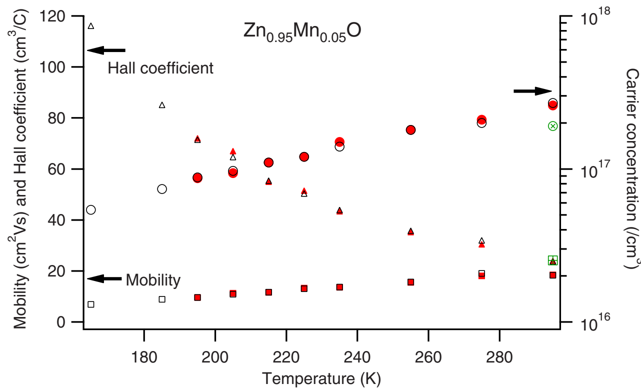

FIG. 6. (Color online) Hall parameters using pin contacts on $Zn_{0.95}Mn_{0.05}O$. Open symbols are 6 T values; closed symbols are 3 T values. Triangles are Hall coefficient, squares are mobility, and circles are carrier concentration. 1 T values (open symbol with crosses) using soldered contacts are shown at room temperature only, and are slightly higher for mobility and slightly lower for carrier concentration.

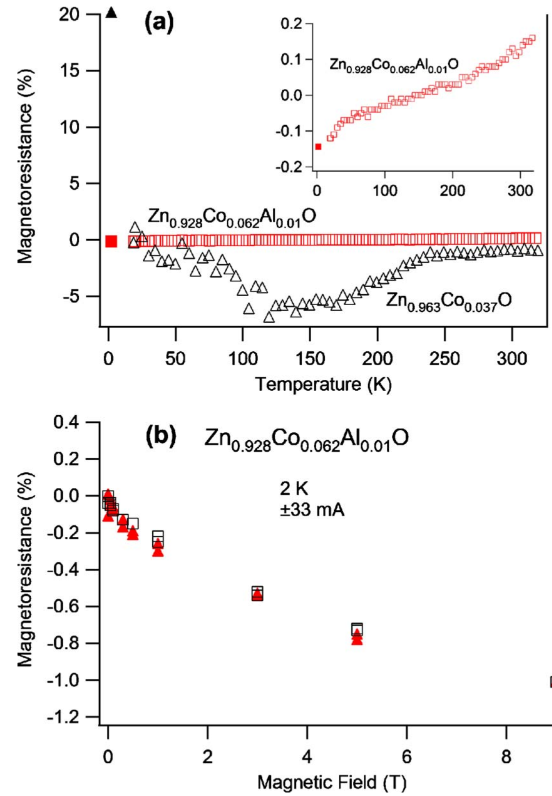

FIG. 7. (Color online) (a) MR vs temperature for $Zn_{0.928}Co_{0.062}Al_{0.01}O$ (squares) and $Zn_{0.963}Co_{0.037}O$ (triangles). Open symbols are from 1 T experiment with soldered contacts and solid symbols are from 2 K experiment at 1 T with pin contacts. Inset shows blowup of $Zn_{0.928}Co_{0.062}Al_{0.01}O$ MR. (b) MR vs magnetic field for $Zn_{0.928}Co_{0.062}Al_{0.01}O$. Solid triangles are data obtained using 33 mA, and open squares are data obtained using −33 mA. Smaller absolute values of currents produced noisier data.

Utilization of spring-loaded contacts is particularly attractive for ultrathin epitaxial films for the following reasons. First, surface damage and contamination is minimized, allowing reuse of films for other purposes. The blunt spring pins also prevent inadvertently punching through any insulating buffer layer film to a more conducting substrate. Solder placement and removal are not required so the film does not undergo repeated localized heating. Additionally, the use of surface contacts allows investigation of films on an insulating substrate, rather than requiring an underlayer and overlayer conductor for through-film transport which could diffuse into the film and affect its chemistry. In this way, the film composition and substrate strain-related effects on conductivity can be carefully studied.

It is estimated that for Ohmic pin contacts, the contact resistances are within a factor of 2 of soldered contacts. The pin contacts remained Ohmic down to low temperatures for most cases. For MR, Hall effect, or anomalous Hall effect measurements, it is important that the pins be nonmagnetic to avoid spurious hysteretic signals.

Additionally, size and shape of the samples were an important consideration, as most of our samples were on substrates of either 5×10 or 10×10 mm dimensions, with the films being somewhat smaller in at least one dimension (Fig. 2). Comparing four-point collinear and VDP configurations, we find the four-point collinear method to be well suited for resistivity and MR measurements, and it requires only one data set rather than two. For four-point collinear measurements, a single pin configuration can be used for any of our samples. For VDP measurements, however, it is desirable to have a pin configuration which places the pins as close as possible to the corners of the sample to avoid large errors, particularly in Hall coefficient. A VDP configuration or equivalent, of course, is necessary if Hall data are sought.

Geometrical corrections (e.g., distance from outer pin to edge of film, etc.) applied to the samples used for the four-point collinear measurements make a difference of at most a factor of 2.[23] VDP geometrical corrections, especially for Hall coefficient, can be large if pins are not placed very near the corners. The relative error for one contact away from the corner of a square samples scales is $(d/D)^4$ for resistivity and $(d/D)^2$ for Hall coefficient, where d is the diagonal distance from the corner to the offset contact and D is the length of the side of the square sample.[24,25] Analyses of errors of con-

TABLE III. Extracted parameters from analysis of Hall data. (Measurements taken six months apart with different setups gave donor and acceptor concentrations which were repeatable to within a factor of at most ~4. It is unclear whether these changes are intrinsic to the material or due to error propagation.)

Material	Carrier concentration (RT, cm^{-3})	Mobility (RT, $cm^2/V\ s$)	Donor concentration (RT, cm^{-3})	Acceptor concentration (RT, cm^{-3})	$k_F l$
$Zn_{0.928}Co_{0.062}Al_{0.01}O$	6.48×10^{20} (LS)	27.6 (LS)	1.06×10^{21} (LS)	4.09×10^{20} (LS)	220 (LS)
	5.40×10^{20} (PPMS)	39 (PPMS)	6.53×10^{20} (PPMS)	1.13×10^{20} (PPMS)	272 (PPMS)
$Zn_{0.963}Co_{0.037}O$	1.67×10^{17} (LS)	18.3 (LS)	⋯	⋯	0.60 (LS)
$Zn_{0.95}Mn_{0.05}O$	1.91×10^{17} (LS)	24.5 (LS)	⋯	⋯	0.87 (LS)
	2.66×10^{17} (PPMS)	18.4 (PPMS)			0.81 (PPMS)

tact placement for VDP measurements generally consider only one of the four contacts being offset, but in one of his original papers, van der Pauw shows that the errors due to multiple contacts being away from the corner are, to a first approximation, additive.[26] For the Hall configuration shown in Fig. 2(b), the error is calculated to be less than 10% on the Hall coefficient. These introduced errors must be considered when designing a pin system where the pins will be close enough to the corners to minimize errors, but not so close that it becomes prohibitively difficult to place them in contact with the film. With very thin and transparent films it can be difficult to distinguish between the film and the polished substrate when trying to carefully align the pin block onto the sample. If surface pads of indium tin oxide or other contact conductors are used with the pins, the VDP geometry is much easier to use than the COL geometry, given the typical close spacings of the pins ($\sim$1 mm) in four-point collinear measurements.

For the square sample where we were able to test both four-point collinear and VDP ($Zn_{0.95}Mn_{0.05}O$), the values agreed within a factor of 2 (Fig. 4). Despite the concerns about the Hall effect errors introduced by the pins, the computed carrier concentrations for the pin contact and soldered measurements are within a factor of 1.5 and the room-temperature resistivities are almost identical. Calculated mobility was about 30% higher for the soldered contacts than the pin contacts.

2. Signal to noise

We have found that MR and resistivity measurements on high resistivity samples are quite difficult to perform due to the small source currents required to achieve measurable voltage drops. Tests are normally performed in constant current mode to ensure stable measurements. The highest currents available using the source meter are limited by the maximum voltage available (210 V). Operation at the highest current possible is desired to increase the voltage measured between pins B and C (Fig. 1). There is noise observed between these pins, and a maximum signal voltage allows for the highest possible signal-to-noise ratio. When the source meter is operating at the maximum supply voltage, it is termed to be in "compliance" and cannot necessarily generate a high enough potential to source the requested current. The actual supplied current, although lower than requested, can be accurately measured and so resistivity can still be determined accurately. Hall effect measurements are more difficult with high resistivity samples since the Hall voltage is typically a small fraction of the voltage drop used for determining resistivity. Reliable Hall measurements, therefore, were not possible for the highest resistivity samples, especially at low temperatures where the resistivity sharply increases. For these reasons, a full set of temperature dependent data (resistivity, carrier concentration, mobility, and MR) were not obtainable with our current setup for the two highest resistivity samples.

It is desirable to maximize the current to get a large voltage for a given resistance while maintaining the source meter within compliance limits (if possible). One example of having the current too small is in the case of the low-temperature MR of $Zn_{0.928}Co_{0.062}Al_{0.01}O$. With ± 3 μA currents, the smallest magnetically induced voltage changes were 0.05 mV, whereas the same MR voltages were 0.5 mV at ± 3.3 mA. This discrepancy resulted in an initial miscalculation of the resistivity since the signal-to-noise ratio was very low at the lowest applied currents.

Similar problems can be encountered in Hall effect measurements, where there may be an apparent, but spurious, change in carrier type (i.e., the Hall coefficient changes sign) or just very noisy data (Fig. 5). This phenomenon occurs due to the averaging of four typically small voltage values (positive and negative fields each at positive and negative currents), where if one of the four data points is spurious, it results in an inaccurate Hall voltage. Here, working at higher fields is helpful as the Hall voltage will be larger (such as in Fig. 6).

3. Special concerns for low and high resistivity samples

Isothermal measurements of low resistivity samples at low temperature have an added complication due to resistive heating of the samples at appreciable currents, leading to temperature instability. It is important to balance the needs of high enough current for good voltage drops but low enough to avoid Joule heating of the sample. In the case of the lowest resistivity sample we tested, $Zn_{0.928}Co_{0.062}Al_{0.01}O$, the relatively high current applied (70.5 mA) for measuring resistivity produced heating at low temperatures, which was initially difficult to diagnose and distinguish from cryostat problems.

We found in measuring the samples of higher resistance that the time constants produced by the capacitance of the $\sim$1 m of unshielded, unguarded cabling inside the PPMS were too long, producing unavoidable voltage transients. This proved problematic especially for MR measurements at low temperature. An improved setup will bypass the PPMS LEMO® cable and all the internal cabling and use shielded coaxial cable up to the top of the Dewar where it will be converted to triaxial cable which goes directly to the electrometers and source meter. The high resistance measurements with our current setup are probably only good to within a factor of 5. However, this is acceptable for many research purposes where order-of-magnitude differences are expected.

4. Magnet considerations

It is important to understand the magnetic field remanence if the field is swept, particularly when doing MR measurements. We found that switching currents without discharging the magnet to zero field resulted in a measured MR that was asymmetric about zero field. This phenomenon is believed to be due to hysteresis in the superconducting magnets, which is in turn dependent upon the charging history of the magnet. We found that with our PPMS system, the field error (reported field-actual field) was less than $\pm 1.5\%$ when the field was ± 0.1 T, $<0.5\%$ at ± 0.2 T, and $<0.2\%$ at ± 1 T. The errors are larger at lower fields; at 0.025 T (250 Oe), field error was $\sim \pm 6\%$. The "zero" field was found to have

the highest absolute deviation from the selected field, about ±20 G, which is acceptable. It was found empirically that directional changes in the current should only be made at zero fields or erroneous data are produced and the MR will not be symmetric with positive and negative fields. It should be noted that this effect is universal. Electromagnet-based systems with large poles can show notoriously large effects, but all systems can show effects due to the magnetic history.

B. Material measurements

1. Resistivity

First, the lowest resistivity sample $Zn_{0.928}Co_{0.062}Al_{0.01}O$ was co-doped with Al to increase conductivity;[8] the various room-temperature resistivity values were all within a factor of ~1.5, with the mean and standard deviation being $3.96 \pm 0.85 \times 10^{-4}$ Ω-cm. Because only a single current value was tested in the PPMS test, it was not possible to verify Ohmic contacts of the pins. However, for the same sample subjected to a 2 K MR test over many currents, the contacts were found to be Ohmic (±3–±3.3 mA). Four-point COL PPMS data were not obtained at 5 K for this sample due to the current being excessively high (70.5 mA), causing Joule heating which could not be overcome by the cryogenic system, so the last recorded datapoint is shown in Table II. As shown in Fig. 2, the decrease in resistivity with temperature is very weak; however, this sample can be described as a degenerate semiconductor with weak metallic character.

The next lowest resistivity sample was vacuum-reduced $Zn_{0.963}Co_{0.037}O$, for which there was a slightly larger distribution of room-temperature resistivities with the various techniques, yielding resistivities in which the extremes differed by a factor of 4.3, with an average and standard deviation of 1.13 ± 0.80 Ω-cm. The conductivity of this sample was increased through postgrowth annealing in vacuum at a temperature of 700 °C. Postgrowth vacuum annealing increases the carrier concentration in TiO_2 and ZnO by the introduction of either oxygen vacancies or metal interstitials (in this case Zn) or both.[8] Pin contacts were confirmed to be Ohmic from room temperature to 5 K. Resistivity sharply increases below ~50 K and was observed to increase by a factor of nearly 200 at 5 K relative to its room-temperature value.

The manganese-doped sample, $Zn_{0.95}Mn_{0.05}O$, was the next most resistive at room temperature. It was measured on the PPMS in both VDP and COL geometries (all pin contacts), and these measurements agreed within a factor of 2 from room temperature to 5 K. Pin contacts were Ohmic above 30 K, and below this the electrometer operated in compliance so the requested current could not be supplied. However, the temperature-dependent resistivity did not produce sharp deviations from one data point to the next, implying that the contacts remained Ohmic throughout the temperature range. The resistivity increased by more than eight orders of magnitude from room temperature to 5 K.

Finally, $Zn_{0.854}Co_{0.146}O$ was the highest resistivity doped sample and was thus the most difficult to measure. The bench-top measurement, which was difficult to obtain, was about a factor of 10 higher than that measured using the PPMS system with pin contacts, exhibiting an average of 6.5×10^2 Ω-cm. For the PPMS data, the contacts were confirmed to be Ohmic down to about 15 K, but the precision of the measurement is questionable below ~50 K as the sheet resistance exceeded 10^{11} Ω/sq and the time constants could become very large. Again, going to a completely guarded system inside the PPMS will be required for adequate measurements below ~100 K for this sample.

A pure, undoped ZnO PLD film was also grown, and it was very resistive. Room-temperature sheet resistances were $\sim 10^9$ Ω/sq (resistivity of $\sim 10^5$ Ω-cm), rising to $\sim 10^{13}$ Ω/sq (resistivity of $\sim 10^9$ Ω-cm) by 100 K, and the contacts remained Ohmic with decreasing temperature.

2. Hall effect

Table III shows carrier parameters extracted from Hall data. For electrons in degenerately doped n-type semiconductors, Matthiessen's rule[27] can be used to separate the mobility contributions from the ionized impurities (charged centers) and the boundary scattering. Boundary-scattering mobility is only dependent on the carrier concentration and film thickness.[28] Ionized-impurity-scattering mobility can be described by the degenerate Brooks–Herring formulation,[27] which depends on the carrier concentration and the ratio of acceptors to donors. This ratio can be found by fitting the measured mobility for the degenerate semiconductor (see, for example, Ref. 13). Hall measurements versus temperature performed on our degenerate sample, $Zn_{0.928}Co_{0.062}Al_{0.01}O$ (Fig. 5), confirmed the assumption of a degenerate, temperature-independent carrier concentration, and validated our use of the degenerate Brooks–Herring formulation for calculating donor and acceptor concentrations.

For the case with degenerate carriers, the mean distance between donors (r) is much smaller than the effective Bohr radius (a_B). A critical electron concentration (n_c) can be computed when these quantities are equal ($r \sim a_B$),[29]

$$n_c = \frac{3/(4\pi)}{a_B^3} = \left(\frac{0.62}{a_B}\right)^3$$

where

$$a_B = (0.53\ \text{Å})\frac{\varepsilon_r}{m_r} \quad \text{since} \quad r = \left(\frac{3}{4\pi n}\right)^{1/3}.$$

For Co:ZnO, the critical concentration of carriers that induces this insulator-to-metal transition has been computed[29] to be $4 \times 10^{19}/\text{cm}^3$. Thus the $Zn_{0.928}Co_{0.062}Al_{0.01}O$ sample is metallic by this criterion and all the other samples should be insulating (see Table III). The product of the Fermi wave vector (k_F) and the mean free path (l) has been shown to be indicative of the degree of electron wave function localization, and can be computed as[30]

$$k_F l = \frac{\hbar(3\pi^2)^{3/2}}{e^2 \rho n^{1/3}}.$$

Hence, knowledge of the resistivity (ρ) and carrier concentration (n) is sufficient to assess whether $k_F l > 1$ (the weakly localized "metallic" regime) or $k_F l < 1$ (the strongly local-

ized "insulating" regime). The latter is associated with higher resistivity, mobility limited at low temperatures by phonon assisted tunneling, large positive MR, and the anomalous Hall effect.[29] Again the data here are consistent with these expectations, with $k_F l \gg 1$ for $Zn_{0.928}Co_{0.062}Al_{0.01}O$ and <1 for $Zn_{0.963}Co_{0.037}O$ and $Zn_{0.95}Mn_{0.05}O$.

3. MR

For the degenerate case where low-temperature mobility is limited by ionized-impurity scattering, the resistivity versus temperature behavior is metallic and decreases slightly as temperature is lowered. Electron wave functions are delocalized, and MR is small and negative.[29] Our low-temperature MR measurements on the metallic $Zn_{0.928}Co_{0.062}Al_{0.01}O$ confirmed this small negative MR [Fig. 7(b)]. However, for higher temperatures, MR was found to be positive [Fig. 7(a)] and can be explained as follows. Even though classical positive MR is not predicted for degenerate electrons, it is still possible due to various mechanisms including multiple electron populations (e.g., surface layer and/or bulk/substrate interface layer), correlated electron-electron interactions, or magnetocrystalline effects.[27] We have observed positive MR in other degenerate ZnO films doped only with Ga and known to be inhomogeneous in depth. We suspect the same mechanism in this case (not shown).

For the semi-insulating $Zn_{0.963}Co_{0.037}O$ with $k_F l < 1$, positive MR is expected. We did observe relatively large positive MR at low temperatures, but small negative MR at room temperature [Fig. 7(a)]. MR as a function of field at low temperature showed complex behavior with both positive and negative MR components (not shown). It is clear from this study and others that the MR behavior in Co:ZnO is very complicated and not easily classified by single parameters such as $k_F l$.

V. CONCLUSIONS

We have measured magnetotransport in Co- and Mn-doped ZnO with various resistivities and found consistent numerical resistivities using multiple methods. We hypothesize that the limitations of our buffered electrometer system are primarily in the time constant, and are due to the capacitance of the unguarded cabling in the Dewar, which we are in the process of bypassing. Pin contacts were shown to be Ohmic and as reliable as soldering. Four-point collinear measurements were found to be adequate and numerically consistent with VDP measurements for resistivity, thus reducing the number of measurements necessary, since MR data can be collected using this geometry. Only Hall effect measurements require the VDP configuration and hence two sets of measurements to determine resistivity. We have demonstrated the use of applied currents between 30 pA and 70 mA to measure samples with room-temperature resistivities of $10^{-4}-10^{5}$ Ω-cm. The current system is limited to sheet resistances of about 10^{13} Ω/sq, at which point the expected precision on resistivity is within a factor of 5. However, under most conditions, measurements from various systems agree to within a factor of 2. Our experience has shown the importance of performing transport measurements using multiple currents, at multiple magnetic fields, and as a function of temperature. This is necessary to assess the validity, repeatability, and inherent errors encountered in taking transport measurements. We have shown that our cobalt-doped ZnO samples lie on either side of the metal-insulator transition as demonstrated by the resistivity as a function of temperature and localization criteria calculations.

ACKNOWLEDGMENTS

This work at PNNL was supported by the U.S. Department of Energy, Office of Science, Division of Materials Sciences and Engineering, and was performed in the Environmental Molecular Sciences Laboratory, a national scientific user facility sponsored by the Department of Energy's Office of Biological and Environmental Research and located at PNNL. PNNL is operated for the U.S. Department of Energy by Battelle under Contract No. DE-AC05-76RL01830. The work at Wright State University (WSU) was supported by AFOSR Grant No. FA9550-07-1-0013, NSF Grant No. DMR0513968, and DOE Grant No. DE-FG02-07ER46389. The authors would also like to thank Daniel Gamelin, Claire Johnson, and Kelly Whitaker for their preparation of the colloidal nanoparticles used to generate some PLD targets, and Tim Cooper for the Hall-effect measurements carried out at WSU.

[1] H. Ohta and H. Hosono, Mater. Today **7**, 42 (2004).
[2] R. B. M. Cross and M. M. De Souza, Appl. Phys. Lett. **89**, 263513 (2006).
[3] E. Fortunato, P. Barquinha, A. Pimentel, A. Goncalves, A. Marques, L. Pereira, and R. Martins, in *Zinc Oxide: A Material for Micro- and Optoelectronic Applications*, edited by N. H. Nickel and E. Terukov (Springer, New York, 2005), p. 225.
[4] W. Fuhs, in *Zinc Oxide: A Material for Micro- and Optoelectronic Applications*, edited by N. H. Nickel and E. Terukov (Springer, New York, 2005), p. 197.
[5] D. S. Ginley and C. Bright, MRS Bull. **25**, 15 (2000).
[6] U. Ozgur, Y. A. Alivov, C. Liu, A. Teke, M. A. Reschchikov, S. Dogan, V. Avrutin, S.-J. Cho, and H. Morkoc, J. Appl. Phys. **98**, 041301 (2005).
[7] T. Dietl, H. Ohno, F. Matsukura, J. Cibert, and D. Ferrand, Science **287**, 1019 (2000).
[8] T. C. Kaspar, T. Droubay, S. M. Heald, P. Nachimuthu, C. M. Wang, V. Shutthanandan, C. A. Johnson, D. R. Gamelin, and S. A. Chambers, New J. Phys. **10**, 055010 (2008).
[9] D. C. Look, D. C. Reynolds, J. R. Sizelove, R. L. Jones, C. W. Litton, G. Cantwell, and W. C. Harsch, Solid State Commun. **105**, 399 (1998).
[10] K. Maeda, M. Sato, I. Niikura, and T. Fukuda, Semicond. Sci. Technol. **20**, S49 (2005).
[11] A. Polyakov, N. Smirnov, A. Govorkov, E. Kozhukhova, S. Pearton, D. Norton, A. Osinsky, and A. Dabiran, J. Electron. Mater. **35**, 663 (2006).
[12] K. G. Saw, K. Ibrahim, Y. T. Lim, and M. K. Chai, Thin Solid Films **515**, 2879 (2007).
[13] D. C. Look, R. L. Jones, J. R. Sizelove, N. Y. Garces, N. C. Giles, and L. E. Halliburton, Phys. Status Solidi A **195**, 171 (2003).
[14] J. J. Chen, Y. Gao, F. Zeng, D. M. Li, and F. Pan, Appl. Surf. Sci. **223**, 318 (2004).
[15] J. Yao and J. Yoon, Rev. Sci. Instrum. **71**, 1776 (2000).
[16] J. R. Drabble and T. D. Whyte, J. Phys. E **3**, 515 (1970).
[17] Keithley, Application Note 2615 (2005).
[18] N. S. Norberg, K. R. Kittilstved, J. E. Amonette, R. K. Kukkadapu, D. A. Schwartz, and D. R. Gamelin, J. Am. Chem. Soc. **126**, 9387 (2004).
[19] D. A. Schwartz, N. S. Norberg, Q. P. Nguyen, J. M. Parker, and D. R. Gamelin, J. Am. Chem. Soc. **125**, 13205 (2003).
[20] L. A. Chick, L. R. Pederson, G. D. Maupin, J. L. Bates, L. E. Thomas, and G. J. Exarhos, Mater. Lett. **10**, 6 (1990).
[21] T. C. Droubay, D. J. Keavney, T. C. Kaspar, S. M. Heald, C. M. Wang, C. A. Johnson, K. M. Whitaker, D. R. Gamelin, and S. A. Chambers, Phys. Rev. B **79**, 155203 (2009).

[22] *Low Level Measurements Handbook: Precision DC Current, Voltage, and Resistance Measurements*, 6th edition (Keithley Instruments, Cleveland, OH, 2004).
[23] D. K. Schroder, *Semiconductor Material and Device Characterization* (IEEE and Wiley-Interscience, Hoboken, NJ, 2006).
[24] D. W. Koon, Rev. Sci. Instrum. **60**, 271 (1989).
[25] D. W. Koon, A. A. Bahl, and E. O. Duncan, Rev. Sci. Instrum. **60**, 275 (1989).
[26] L. J. van der Pauw, Philips Res. Rep. **13**, 1 (1958).
[27] D. C. Look, *Electrical Characterization of GaAs Materials and Devices* (Wiley, Chichester, 1989).
[28] D. C. Look, K. D. Leedy, D. H. Tomich, and B. Bayraktarolgu, Appl. Phys. Lett. **96**, 062102 (2010).
[29] Q. Xu, L. Hartmann, H. Schmidt, H. Hochmuth, M. Lorenz, R. Schmidt-Grund, C. Sturm, D. Spemann, and M. Grundmann, Phys. Rev. B **73**, 205342 (2006).
[30] Q. Xu, L. Hartmann, H. Schmidt, H. Hochmuth, M. Lorenz, D. Spemann, and M. Grundmann, Phys. Rev. B **76**, 134417 (2007).